

Theoretical investigation on vibration frequency of sandwich plate with PFRC core and piezomagnetic face sheets under variable in-plane load

Ali Ghorbanpour Arani*, Zahra Khoddami Maraghi^a and Maryam Ferasatmanesh^b

Department of Solid Mechanics, Faculty of Mechanical Engineering, 6Km Ghotbravandi Blvd, University of Kashan, Kashan, Iran

(Received July 3, 2016, Revised January 5, 2017, Accepted January 25, 2017)

Abstract. This research investigated the vibration frequency of sandwich plate made of piezoelectric fiber reinforced composite core (PFRC) and face sheets of piezomagnetic materials. The effective electroelastic constants for PFRC materials are obtained by the micromechanical approach. The resting medium of sandwich plate is modeled by Pasternak foundation including normal and shear modulus. Besides, sandwich plate is subjected to linearly varying normal stresses that change by load factor. The coupled equations of motion are derived using first order shear deformation theory (FSDT) and energy method. These equations are solved by differential quadrature method (DQM) for simply supported boundary condition. A detailed numerical study is carried out based on piezoelectricity theory to indicate the significant effect of load factor, volume fraction of fibers, modulus of elastic foundation, core-to-face sheet thickness ratio and composite materials on dimensionless frequency of sandwich plate. These findings can be used to aerospace, building and automotive industries.

Keywords: composites; fiber reinforced; numerical method; plate structures; dynamic analysis

1. Introduction

In the recent decades the sandwich structures has been widely used for applications ranging such as aircraft, ships, satellites, rail cars, automobiles, wind energy systems, marine and building constructions because of their low specific weight, high dynamic characteristics, outstanding banding rigidity and maximum fatigue properties (Lal and Rani 2014).

Fiber-reinforced composite materials include fibers of high strength and modulus embedded in or bonded to a matrix with distinct interfaces between them. In this combination, both fibers and matrix maintain their chemical and physical properties, while they have not these features alone (Mallick 2007). The fiber-reinforced composite laminates have many advantages like high stiffness -to-weight ratio, high strength-to-weight ratio, corrosion resistance properties, good fatigue resistance properties etc. So, these laminates are widely employed in the design of structural components in cars, rail vehicle, robots, power plants etc. (Aravinda Kumar *et al.* 2015).

Zhang and Sun (1999) studied a sandwich plate containing a piezoelectric core. They used the principle of stationary potential energy and Raleigh-Ritz formulation for

the sandwich plate. They analyzed this problem by Finite element method. Benjeddou and Deu (2002) presented a two-dimensional (2D) closed-form solution for the free vibrations analysis of simply supported piezoelectric sandwich plates. In this work, FSDT and through-thickness quadratic electric potential were considered for layers. Micromechanic models for non-linear behavior of PFRC was discussed by Tong and Tan (2001, 2002). They exhibited two non-linear micromechanics models, namely, "XY PFRC non-linear model" and "YX PFRC non-linear model". Also, they presented two micromechanic models, referred to as "XY PEMFRC model" and "YX PEMFRC model" to calculate the electro-magneto-thermo-elastic properties for piezoelectric-magnetic fiber reinforced composite (PEMFRC) materials. Nayak and *et al.* (2002) investigated free vibration analysis of composite sandwich plates based on Reddy's higher-order theory to determine the natural frequencies of isotropic, orthotropic, and layered anisotropic composite and sandwich plates. They used glass fiber polyester resins for the face sheets and poly-vinyl-chloride (PVC) for the core of sandwich. Consistent higher-order free vibration analysis of composite sandwich plates was developed by Wang *et al.* (2008). They obtained eight dynamic governing equations and the corresponding boundary conditions by the application of Hamilton's principle. Their results showed that the vibration modes of the soft-core sandwich plates with symmetric and anti-symmetric layups. Iu *et al.* (2008) studied free vibration of functionally graded material (FGM) sandwich rectangular plates with simply supported and clamped edges based on the three-dimensional linear theory of elasticity. They considered two types of FGM sandwich plates, the sandwich with homogeneous face sheet and FGM core and the sandwich with FGM face sheet and homogeneous core.

*Corresponding author, Professor
E-mail: aghorban@kashanu.ac.ir,
a_ghorbanpour@yahoo.com

^aPh.D.
E-mail: Z.Khoddami@gmail.com

^bMSc Student
E-mail: M.ferasatmanesh@gmail.com

They obtained the natural frequencies using the Ritz method. Their results revealed that the number of thickness expansion terms mainly depends on the thickness of the plate. Finite element modeling for bending and vibration analysis of laminated and sandwich composite plates based on higher-order theory was presented by Tu *et al.* (2010). They solved the problem with existing numerical solutions. They presented the results for the parametric effects of degree of orthotropy, length-to-thickness ratio, plate aspect ratio upon the fundamental frequencies. A finite element model for analyzing of active sandwich laminated plates was presented by Araújo *et al.* (2010) with a viscoelastic core and laminated anisotropic face layers, as well as piezoelectric sensor and actuator layers. They used FSDT for the displacement field of the adjacent laminated anisotropic face layers and exterior piezoelectric layers, and a higher order shear deformation theory (HSDT) to represent the displacement field of the viscoelastic core. Their model was capable of handling a wide variety of layer configurations. They have also implemented the velocity feedback control laws. Vel *et al.* (2012) analyzed the fiber-reinforced composite plates integrated piezoceramic fiber composite actuators. They solved the three-dimensional macroscopic equilibrium equations for a laminated piezoelectric plate using the Eshelby-Stroh formalism. They presented the results for the homogenized material properties, macroscale average stresses, macroscale deformation and microscale stress distributions. Wang and Shen (2012) analyzed nonlinear vibration and bending of sandwich plates with carbon nanotube-reinforced composite (CNTRC) face sheets resting on an elastic foundation in thermal environments. They considered the material properties of CNTRC face sheets graded in the thickness direction. They solved the governing equation of the plate including plate-foundation interaction by a two-step perturbation technique. Their findings showed that the linear functionally graded (FG) reinforcement of face sheets has a quantitative effect on the nonlinear bending behaviors. They also found that the temperature rise and foundation stiffness have a significant effect on the natural frequencies, and nonlinear bending behaviors of the sandwich plate. Hadji and Adda Bedia (2012) analyzed the behavior of FG beams based on neutral surface position. They presented the n -order polynomial term for the displacement field without shear correction factor. In this theory, transverse shear stress variation varied parabolically across the thickness satisfying shear stress free surface conditions. A novel higher order shear and normal deformation theory based on neutral surface position for bending analysis of advanced composite plates was done by Bousahla *et al.* (2013). The number of unknown functions involved in the present theory was only five as against six or more in case of other shear and normal deformation theories. They used the principle of virtual work and the physical neutral surface concept to obtain the governing equations. Thermo-mechanical bending response of FGM thick plates resting on Winkler-Pasternak elastic foundations was presented by Boudierba *et al.* (2013). They assumed the material properties of the FG plates varied continuously through the thickness, according to a simple power law distribution of

the volume fraction. Analysis of FG sandwich plate with piezoelectric skins was done by Loja *et al.* (2013) using B-spline finite strip method. They used different shear deformation theories to study the static and free vibration behavior of FG sandwich plate. They also computed the effective properties of FGMs based on Mori-Tanaka homogenization scheme. A new higher-order shear and normal deformation theory for the bending and free vibration analysis of sandwich plates with FG isotropic face sheets was investigated by Bessaim *et al.* (2013). Their theory had five numbers of unknown functions as against six or more in case of other shear and normal deformation theories. They considered simply support boundary condition in all edges and the plate subjected to a sinusoidally distributed load. They used Hamilton's principle for obtaining the equations of motion. Houari *et al.* (2013) studied a new higher order shear and normal deformation theory to simulate the thermoelastic bending of FGM sandwich plates. They used the exact solution for a simply-supported FGM sandwich plates. Their results showed that the proposed higher order shear and normal deformation theory is not only accurate but also provided an elegant and easily implementable lends approach for simulating thermoelastic bending behavior of FG sandwich plates. A refined trigonometric shear deformation theory for thermo-elastic bending of FG sandwich plates was presented by Tounsi *et al.* (2013). In this paper, the number of unknown functions involved was only four and did not require shear correction factor. This theory satisfies shear stress free surface conditions because the transverse shear stresses vary parabolically across the thickness of plate. The effects of transverse shear deformation, thermal load, plate aspect ratio and volume fraction distribution were investigated in the paper. Bennoun *et al.* (2014) were presented a novel five-variable refined plate theory for vibration analysis of FG sandwich plates. Indeed, in their theory the number of unknown functions was only five. Their results revealed that the proposed theory is accurate and efficient in predicting the free-vibration response of FG sandwich plates. An efficient and simple refined theory for buckling and free vibration of exponentially graded sandwich plates under various boundary conditions was investigated by Ait Amar Meziane *et al.* (2014). They used the Hamilton's principle to obtain the equations of motion. Theory could archive accuracy comparable to the existing HSDTs that contain more number of unknowns. New quasi-3D hyperbolic shear deformation theory for the static and free vibration analysis of FG plates was presented by Hebali *et al.* (2014). They divided the transverse displacement into bending, shear, and thickness stretching parts. Also the number of unknowns and governing equations of the present theory was reduced. A new hyperbolic shear deformation theory applicable to bending and free vibration analysis of isotropic, FG, sandwich and laminated composite plates was presented by Mahi *et al.* (2014). Their new theory had five degrees of freedom, provided parabolic transverse shear strains across the thickness direction and hence, it did not need shear correction factor. They used the Hamilton's principle for the energy functional of the system. Their results showed that the present theory can be

considered as a good alternative to some 2D theories for approximating the tedious and composite. Natarajan and *et al.* (2014) studied the bending and free flexural vibration behavior of sandwich plates with carbon nanotube (CNT) reinforced face sheets using higher-order structural theory. They solved this problem by QUAD-8 shear flexible element. The results of this work showed the influence of the volume fraction of CNT, core-to-face sheet thickness and the plate thickness ratio on sandwich plates. They also found that increasing of the volume fraction of CNT distribution in the face sheet, in general, decreases the deflection of sandwich plates. Belabed *et al.* (2014) were presented an efficient and simple higher order shear and normal deformation theory for FG plates. They calculated the bending, shear and thickness stretching parts in the transverse displacement and decreased the number of unknowns to five. Biaxial wrinkling analysis of composite-faced sandwich plates with soft core using improved high-order theory was investigated by Khalili *et al.* (2014). They used the nonlinear Von-Karman type relations to obtain strains. The equations of motion and boundary conditions were derived by principle of minimum potential energy. They solved this problem by analytical solution for static analysis of simply supported sandwich plates under biaxial in-plane compressive loads using Navier's solution. Their results showed that in constant geometrical parameters, the dimensionless wrinkling loads decrease with increase in the load ratio. Plagianakos and Papadopoulos (2015) analyzed the higher-order 2D/3D layerwise mechanics and finite elements for composite and sandwich composite plates with piezoelectric layers. They solved the governing equation of the plate with Navier solutions and finite element approximations. A new simple shear and normal deformations theory for FG beams was presented by Bourada *et al.* (2015). In this paper, the thickness stretching effect was also included with only 3 unknowns. Yahia *et al.* (2015) were presented Wave propagation in FG plates with porosities using various higher-order shear deformation plate theories. They used the rule of mixture to describe and approximate material properties of the FG plates with porosity phases. Bellifa *et al.* (2016) analyzed the bending and free vibration of FG plates using a simple shear deformation theory and the concept the neutral surface position. They used FSDT and the physical neutral surface concept to obtain the governing equations.

Use of piezoelectric materials as distributed sensors and actuators, has been significantly increasing during the past decade for active control of vibration of high performing lightweight smart structures. Direct and converse piezoelectric effects of piezoelectric materials help the sandwich structure to be used as distributed sensors and actuators. PFRC is one of the new materials in the collection of smart materials that used in this research and integrated with piezomagnetic layer as an intelligent sandwich. Also linearly varying in-plane load are applied on this structure to evaluate the vibrational behavior of sandwich in different positions that hasn't already been done.

This research is distinct from other above papers due to vibration study of sandwich plate:

- ❖ With composite core made of polymer matrix and piezo fibers.
- ❖ Made of piezomagnetic face sheets.
- ❖ Under linearly varying normal stresses.
- ❖ Considering Pasternak foundation.
- ❖ With different matrix and face sheets materials.
- ❖ Solved by 2D DQM.

Free vibration of composite sandwich plate made of two smart piezomagnetic face sheets is a new topic which cannot be found in literature. Magneto-mechanical coupling in piezomagnetic materials feels a connection between stress and magnetic field that can be used in stability of systems. In this research, variable in-plane load are applied on smart sandwich plate where load factor changes the effectiveness of linearly variable in-plane forces from pure comparison to pure bending. Also, core of sandwich is made of PFRC and the effects of material properties of fibers, matrix and face sheets are studied on vibration frequency of sandwich plate. Besides, Pasternak foundation is developed by evaluating of normal and shear modulus. The results of this study investigate the effect of important parameters on vibration frequency of sandwich plate that can be useful in many industries.

2. Constitutive of the sandwich structure

A schematic diagram of a sandwich plate is illustrated in Fig. 1 in which geometrical parameters of length a , width b and thickness $2h_s+h_c$ are also indicated.

As shown in Fig. 1 the sandwich plate is composed of three layers:

1. Central composite core reinforced by piezoelectric fibers,
2. Two face sheets made of piezomagnetic material.

The strain-displacement relations are separately written for each layer, then forces and moments are obtained. Finally the total energy including the energy of PFRC core and piezomagnetic face sheet is obtained. The equations of motion are derived using Hamilton's principle considering variable in-plane forces.

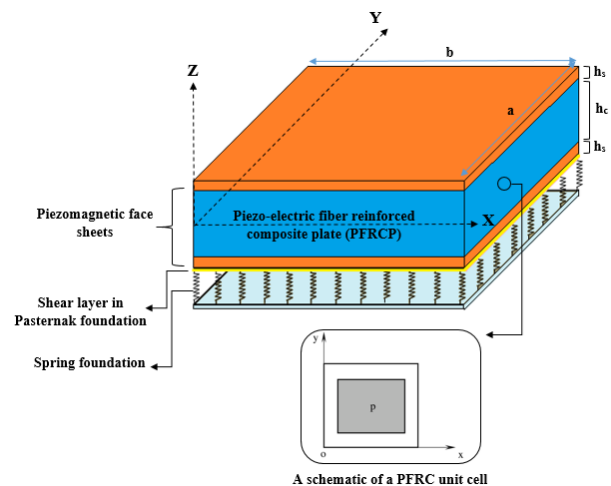


Fig. 1 A schematic diagram of a sandwich PFRC plate

2.1 Composite core

In this research, the central core is a composite reinforced with piezoelectric fibers. Generally, the mechanical constitutive relations of composite material are expressed in Eq. (1)

$$\begin{bmatrix} \sigma_{xx}^c \\ \sigma_{yy}^c \\ \sigma_{zz}^c \\ \sigma_{xy}^c \\ \sigma_{xz}^c \\ \sigma_{yz}^c \end{bmatrix} = \begin{bmatrix} Q_{11} & Q_{12} & Q_{13} & 0 & 0 & 0 \\ Q_{12} & Q_{22} & Q_{23} & 0 & 0 & 0 \\ Q_{13} & Q_{23} & Q_{33} & 0 & 0 & 0 \\ 0 & 0 & 0 & Q_{44} & 0 & 0 \\ 0 & 0 & 0 & 0 & Q_{55} & 0 \\ 0 & 0 & 0 & 0 & 0 & Q_{66} \end{bmatrix} \begin{bmatrix} \varepsilon_{xx} \\ \varepsilon_{yy} \\ \varepsilon_{zz} \\ \varepsilon_{xy} \\ \varepsilon_{xz} \\ \varepsilon_{yz} \end{bmatrix} - \begin{bmatrix} 0 & 0 & e_{31} \\ 0 & 0 & e_{32} \\ 0 & 0 & e_{32} \\ 0 & e_{24} & 0 \\ e_{15} & 0 & 0 \\ 0 & 0 & 0 \end{bmatrix} \begin{bmatrix} E_x \\ E_y \\ E_z \end{bmatrix} \quad (1a)$$

$$\begin{bmatrix} D_x \\ D_y \\ D_z \end{bmatrix} = \begin{bmatrix} 0 & 0 & 0 & 0 & e_{15} & 0 \\ 0 & 0 & 0 & 0 & e_{24} & 0 \\ e_{31} & e_{32} & e_{33} & 0 & 0 & 0 \end{bmatrix} \begin{bmatrix} \varepsilon_{xx} \\ \varepsilon_{yy} \\ \varepsilon_{zz} \\ \varepsilon_{xy} \\ \varepsilon_{xz} \\ \varepsilon_{yz} \end{bmatrix} + \begin{bmatrix} \varepsilon_{11} & 0 & 0 \\ 0 & \varepsilon_{22} & 0 \\ 0 & 0 & \varepsilon_{33} \end{bmatrix} \begin{bmatrix} E_x \\ E_y \\ E_z \end{bmatrix} \quad (1b)$$

Where c is core and σ_{ij} , ε_{ij} and Q_{ij} are the normal and shear stresses, strains and stiffness constants, respectively. Also, D_m , E_n , $e_{\alpha\beta}$ and δ_{mn} are the electric displacement, electric field the piezoelectric constants and the dielectric constants, respectively.

Thermal behavior of materials is a broader subject, more directly related to their general thermal properties than to thermal effects of specific interest. Thermal effects can be calculated according to Refs. (Tounsi *et al.* 2013, Zidi *et al.* 2014, Boudierba *et al.* 2013, Hamidi *et al.* 2015). In this way thermal stresses are added to Eq. (1a) as $[\lambda_{xx} \lambda_{yy} \lambda_{zz} \lambda_{xy} \lambda_{xz} \lambda_{yz}]^T \Delta T$ where λ_{ij} and ΔT are thermal expansion and thermal increment. Also $[\kappa_x \kappa_y \kappa_z]^T \Delta T$ were added to Eq. (1b) in which κ_m is pyroelectric coefficient.

In order to obtain the properties of composite core, a representative volume element (RVE) is considered and "XY-PEFRC" or "YX-PEFRC" known as (Loja *et al.* 2013, Bessaim *et al.* 2013) is employed. Since piezoelectric polymer matrix and piezoelectric reinforcements are assumed to be the smart components, so micromechanical method is used to determine the effective electro-elastic constants for PFRFC materials. The constitutive equations for the electro-thermo-mechanical behavior of selected RVE according to the XY-PEFRC micromechanical method are expressed as (Wang *et al.* 2008)

$$Q_{11} = \frac{\rho Q_{11}^p Q_{11}^m}{\rho Q_{11}^m + (1-\rho) Q_{11}^p}, Q_{12} = Q_{11} \left[\frac{\rho Q_{12}^p}{Q_{11}^p} + \frac{(1-\rho) Q_{12}^m}{Q_{11}^m} \right], a$$

$$Q_{13} = Q_{11} \left[\frac{\rho Q_{13}^p}{Q_{11}^p} + \frac{(1-\rho) Q_{13}^m}{Q_{11}^m} \right]$$

$$Q_{22} = \rho Q_{22}^p + (1-\rho) Q_{22}^m + \frac{Q_{12}^2}{Q_{11}} - \frac{\rho(Q_{12}^p)^2}{Q_{11}^p} - \frac{(1-\rho)(Q_{12}^m)^2}{Q_{11}^m}$$

$$Q_{23} = \rho Q_{23}^p + (1-\rho) Q_{23}^m + \frac{Q_{12} Q_{13}}{Q_{11}} - \frac{\rho Q_{12}^p Q_{13}^p}{Q_{11}^p} - \frac{(1-\rho) Q_{12}^m Q_{13}^m}{Q_{11}^m}$$

$$Q_{33} = \rho Q_{33}^p + (1-\rho) Q_{33}^m + \frac{Q_{31}^2}{Q_{11}} + \frac{\rho(Q_{13}^p)^2}{Q_{11}^p} - \frac{(1-\rho)(Q_{13}^m)^2}{Q_{11}^m}$$

$$Q_{44} = \rho Q_{44}^p + (1-\rho) Q_{44}^m, Q_{66} = \frac{\rho Q_{66}^p Q_{66}^m}{\rho Q_{66}^m + (1-\rho) Q_{66}^p}$$

$$Q_{55} = \frac{A}{B^2 + AC} \rightarrow \begin{cases} A = \frac{\rho Q_{55}^p}{(e_{15}^p)^2 + Q_{55}^p \varepsilon_{11}^p} + \frac{(1-\rho) Q_{55}^m}{(e_{15}^m)^2 + Q_{55}^m \varepsilon_{11}^m} \\ B = \frac{\rho e_{15}^p}{(e_{15}^p)^2 + Q_{55}^p \varepsilon_{11}^p} + \frac{(1-\rho) e_{15}^m}{(e_{15}^m)^2 + Q_{55}^m \varepsilon_{11}^m} \\ C = \frac{\rho \varepsilon_{11}^p}{(e_{15}^p)^2 + Q_{55}^p \varepsilon_{11}^p} + \frac{(1-\rho) \varepsilon_{11}^m}{(e_{15}^m)^2 + Q_{55}^m \varepsilon_{11}^m} \end{cases} \quad (2)$$

$$e_{31} = Q_{11} \left[\frac{\rho e_{31}^p}{Q_{11}^p} + \frac{(1-\rho) e_{31}^m}{Q_{11}^m} \right], e_{24} = \rho e_{24}^p + (1-\rho) e_{24}^m,$$

$$e_{15} = \frac{\rho e_{15}^p e_{15}^m}{\rho e_{15}^m + (1-\rho) e_{15}^p}$$

$$e_{32} = \rho e_{32}^p + (1-\rho) e_{32}^m + \frac{Q_{12} e_{31}}{Q_{11}} - \frac{\rho Q_{12}^p e_{31}^p}{Q_{11}^p} - \frac{(1-\rho) Q_{12}^m e_{31}^m}{Q_{11}^m}$$

$$e_{33} = \rho e_{33}^p + (1-\rho) e_{33}^m + \frac{Q_{13} e_{31}}{Q_{11}} - \frac{\rho Q_{13}^p e_{31}^p}{Q_{11}^p} - \frac{(1-\rho) Q_{13}^m e_{31}^m}{Q_{11}^m}$$

where "p" and "m" indexes refer to piezofiber and matrix and ρ is the volume fraction of fibers. The electric field that is defined as a function of electric potential

$$E_n = -\nabla \cdot \varphi, \quad \nabla = \frac{\partial}{\partial x} i + \frac{\partial}{\partial y} j \quad (3)$$

where φ is the electric potential.

2.2 Piezomagnetic face sheets

In this section, piezomagnetic face sheets are analyzed. Piezomagnetic materials are active materials and possess the effect, i.e., the induced strain is proportional to the applied magnetic field (Jalili 2009). The stress-strain field for face sheets layer is given as

$$\begin{bmatrix} \sigma_{xx}^f \\ \sigma_{yy}^f \\ \sigma_{zz}^f \\ \sigma_{xy}^f \\ \sigma_{xz}^f \\ \sigma_{yz}^f \end{bmatrix} = \begin{bmatrix} C_{11} & C_{12} & C_{13} & 0 & 0 & 0 \\ C_{12} & C_{22} & C_{23} & 0 & 0 & 0 \\ C_{13} & C_{23} & C_{33} & 0 & 0 & 0 \\ 0 & 0 & 0 & C_{44} & 0 & 0 \\ 0 & 0 & 0 & 0 & C_{55} & 0 \\ 0 & 0 & 0 & 0 & 0 & C_{66} \end{bmatrix} \begin{bmatrix} \varepsilon_{xx} \\ \varepsilon_{yy} \\ \varepsilon_{zz} \\ \varepsilon_{xy} \\ \varepsilon_{xz} \\ \varepsilon_{yz} \end{bmatrix} - \begin{bmatrix} 0 & 0 & q_{31} \\ 0 & 0 & q_{32} \\ 0 & 0 & q_{32} \\ 0 & q_{24} & 0 \\ q_{15} & 0 & 0 \\ 0 & 0 & 0 \end{bmatrix} \begin{bmatrix} H_x \\ H_y \\ H_z \end{bmatrix} \quad (4)$$

$$\begin{bmatrix} B_x \\ B_y \\ B_z \end{bmatrix} = \begin{bmatrix} 0 & 0 & 0 & 0 & q_{15} & 0 \\ 0 & 0 & 0 & q_{24} & 0 & 0 \\ q_{31} & q_{32} & q_{33} & 0 & 0 & 0 \end{bmatrix} \begin{bmatrix} \varepsilon_{xx} \\ \varepsilon_{yy} \\ \varepsilon_{zz} \\ \varepsilon_{xy} \\ \varepsilon_{xz} \\ \varepsilon_{yz} \end{bmatrix} + \begin{bmatrix} \mu_{11} & 0 & 0 \\ 0 & \mu_{22} & 0 \\ 0 & 0 & \mu_{33} \end{bmatrix} \begin{bmatrix} H_x \\ H_y \\ H_z \end{bmatrix}$$

Where f is face sheets and B_m and H_n are the magnetic flux and magnetic field, respectively, $q_{\alpha\beta}$ and μ_{mn} are the piezomagnetic coefficients and the magnetic permeability, respectively. C_{ij} is defined according to the elastic stiffness matrix of isotropic materials (Ghorbanpour Arani and Khoddami Maraghi 2015)

$$\begin{aligned} C_{11} = C_{22} &= \frac{E}{(1-\nu^2)}, \quad C_{12} = C_{13} = \frac{E\nu}{(1-\nu^2)}, \\ C_{44} = C_{55} &= \frac{E}{(1+\nu)}, \quad C_{66} = \frac{E}{(1+\nu)} \end{aligned} \quad (5)$$

where E and ν are the Young modulus and Poisson's ratio. Similar to electric field, it can be defined the magnetic field as function of magnetic potential (ψ), as below

$$H_n = -\nabla \cdot \psi \quad (6)$$

3. Equations of motion

The FSDT extends the kinematics of the classical plate theory (CPT) by including a gross transverse shear deformation in its kinematic assumptions. The transverse shear strain is assumed to be constant in FSDT with respect to the thickness coordinate (Wang *et al.* 2000).

Shear correction factors ($k_f=5/6$) are introduced to correct the discrepancy between the actual transverse shear force distributions and those computed using the kinematic relations of the FSDT. The shear correction factors depend on the geometric parameters, loading and boundary conditions of the plate. According to the FSDT for the plate, the displacement field is taken as (Wang *et al.* 2000)

$$\begin{aligned} U(x, y, z, t) &= u_0(x, y, t) + z\theta_1(x, y, t) \\ V(x, y, z, t) &= v_0(x, y, t) + z\theta_2(x, y, t) \\ W(x, y, z, t) &= w_0(x, y, t) \end{aligned} \quad (7)$$

where U, V, W are the displacements of an arbitrary point of the plate along the x, y and z axis, respectively; u_0 and v_0 are mid-plane displacements of x, y axis, and z is a distance between the point and the mid-plane and $\theta_1(x, y, t), \theta_2(x, y, t)$ are rotations about y and x axis and t is time.

The linear strain field for FSDT obtained by using Hooke's law, can be given as

$$\begin{aligned} \varepsilon_{xx} &= \frac{\partial}{\partial x} u_0(x, y, t) + z \frac{\partial}{\partial x} \theta_1(x, y, t) \\ \varepsilon_{yy} &= \frac{\partial}{\partial y} v_0(x, y, t) + z \frac{\partial}{\partial y} \theta_2(x, y, t) \\ \varepsilon_{zz} &= 0 \\ \varepsilon_{xy} &= \frac{1}{2} \left(\frac{\partial}{\partial x} v_0(x, y, t) + z \frac{\partial}{\partial x} \theta_2(x, y, t) + \frac{\partial}{\partial y} u_0(x, y, t) + z \frac{\partial}{\partial y} \theta_1(x, y, t) \right) \\ \varepsilon_{xz} &= \frac{1}{2} k_f \left(\frac{\partial}{\partial x} w_0(x, y, t) + \theta_1(x, y, t) \right) \\ \varepsilon_{yz} &= \frac{1}{2} k_f \left(\frac{\partial}{\partial y} w_0(x, y, t) + \theta_2(x, y, t) \right) \end{aligned} \quad (8)$$

3.1 Energy method in sandwich plate

The energy method is used to obtain the governing equation. The total potential energy (Π) of sandwich plate is the sum of strain energy (U), kinetic energy (K) and the external work (W_E). Strain energy of the rectangular sandwich plate is calculated as (Reddy 2000)

$$\begin{aligned} U &= \frac{1}{2} \int_V (\sigma_{xx}\varepsilon_{xx} + \sigma_{yy}\varepsilon_{yy} + \sigma_{zz}\varepsilon_{zz} + \tau_{xy}'\gamma_{xy} + \tau_{xz}'\gamma_{xz} \\ &\quad + \tau_{yz}'\gamma_{yz} - D_m E_n - B_m H_n) dV \\ U_{sandwich} &= U_{core} + U_{facesheets} \\ &= \frac{1}{2} \int_{-\frac{h_c}{2}}^{\frac{h_c}{2}} \int_0^a \int_0^b (\sigma_{ij}^c \varepsilon_{ij}^c + \tau_{ij}'^c \gamma_{ij}'^c - D_m E_n)_{Core} dx dy dz \\ &\quad + \frac{1}{2} \int_{-\frac{h_m}{2}}^{\frac{h_m}{2}} \int_0^a \int_0^b (\sigma_{ij}^f \varepsilon_{ij}^f + \tau_{ij}'^f \gamma_{ij}'^f - B_m H_n)_{Sheet} dx dy dz \\ &\quad + \frac{1}{2} \int_{\frac{h_c}{2}}^{\frac{h_c}{2} + h_m} \int_0^a \int_0^b (\sigma_{ij}^f \varepsilon_{ij}^f + \tau_{ij}'^f \gamma_{ij}'^f - B_m H_n)_{Sheet} dx dy dz \end{aligned} \quad (9)$$

Substituting Eqs. (1)-(4)-(8) into Eq. (9), the strain energy of the sandwich plate can be obtained.

Also, the kinetic energy of sandwich plate can be stated as

$$\begin{aligned} K_{Sandwich} &= K_{Core} + K_{Face sheets} = \\ &= \frac{1}{2} (\rho_c h_c + 2\rho_f h_f) \left(\int_0^b \int_0^a \left[\left(\frac{\partial \tilde{U}}{\partial t} \right)^2 + \left(\frac{\partial \tilde{V}}{\partial t} \right)^2 + \left(\frac{\partial \tilde{W}}{\partial t} \right)^2 \right] dx dy \right) \end{aligned} \quad (10)$$

in which, ρ_f, ρ_c and h_f, h_c are the density and thickness of core and face sheets.

3.2 Elastic medium

Pasternak foundation model is capable to consider the transverse shear and normal loads (Ghorbanpour Arani *et al.* 2012). In this paper the bottom surface of sandwich plate is continuously supported by an elastic foundation as (Kutlu and Hakkı Omurtag 2012)

$$F = K_w W - K_g \left(\frac{\partial^2 W}{\partial x^2} + \frac{\partial^2 W}{\partial y^2} \right) \quad (11)$$

in which, K_w, K_g are Winkler and shear foundation parameters. Therefore, the external work due to orthotropic elastic foundation is calculated as

$$W_E = \frac{1}{2} \int_0^b \int_0^a F W dx dy \quad (12)$$

3.3 Linearly varying in-plane load

Rectangular plates are usually subjected to in-plane forces, therefore the in-plane stresses effects must be considered in their analysis. Linearly varying in-plane load N_x is applied in x direction as shown in Fig. 2 and it is assumed at the following form (Farajpour *et al.* 2012)

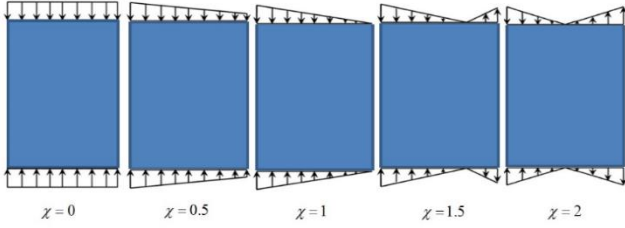


Fig. 2 Linearly varying in-plane load

$$\tilde{N}_x = -N_x \left(1 - \chi \frac{y}{b}\right) \quad (13)$$

where χ is introduced as load factor. The potential energy due to the in-plane force per unit length in the x direction can be written as (An and Su 2014)

$$U_N = \frac{1}{2} \int_0^b \int_0^a \left(N_x \left(\frac{\partial W}{\partial x} \right)^2 \right) dx dy \quad (14)$$

3.4 Hamilton's principle

Hamilton's principle is used herein to derive the equations of motion. The principle can be stated in an analytical form as

$$0 = \int_0^T (\delta U + \delta W_E + \delta U_N - \delta K) dt \quad (15)$$

where δU , δK , δW_E and δU_N are the variation of strain energy, variation of kinetic energy, variation of external work and in-plane force. Substituting Eqs. (9)-(14)-(12) into Eq. (15) for FSDT and afterward using dimensionless parameters which introduced in Eq. (16)

$$(\zeta, \eta) = \left(\frac{x}{a}, \frac{y}{b} \right), (U, V, W) = \left(\frac{u_0}{a}, \frac{v_0}{b}, \frac{w_0}{h_s} \right) \rightarrow$$

$$\text{For } \begin{cases} \text{core} = h_c \\ \text{face sheets} = h_s \end{cases}, (\alpha_s, \beta_s) = \left(\frac{h_s}{a}, \frac{h_s}{b} \right),$$

$$(\alpha_c, \beta_c) = \left(\frac{h_c}{a}, \frac{h_c}{b} \right), \delta = \frac{h_c}{h_s}, \gamma = \frac{a}{b}$$

(16)

$$(\psi, \psi_1, \psi_2) = \left(\frac{q_{24}}{q_{15}}, \frac{q_{31}}{q_{15}}, \frac{q_{32}}{q_{15}} \right), (\lambda, \lambda_1, \lambda_2) = \left(\frac{e_{15}}{e_{24}}, \frac{e_{31}}{e_{24}}, \frac{e_{32}}{e_{24}} \right)$$

$$\left(\frac{h_c}{2} + h_s \right) = Z \rightarrow \frac{Z}{h_s} = \bar{Z}, \bar{\rho} = \frac{\rho_c}{\rho_s},$$

$$\bar{\varphi} = \frac{\varphi e_{24}}{Q_{11} a}, \bar{s} = \frac{s q_{15}}{C_{11} a} \tau = \frac{t}{a} \sqrt{\frac{C_{11}}{\rho_s}},$$

$$(\bar{\epsilon}_{22}, \bar{\epsilon}_{33}) = \begin{pmatrix} \epsilon_{22} & \epsilon_{33} \\ \epsilon_{11} & \epsilon_{11} \end{pmatrix}, Y = \frac{\mu_{11} E_s}{q_{15}^2}, g = \frac{\epsilon_{11} Q_{11}}{e_{24}^2}$$

$$(\bar{\mu}_{22}, \bar{\mu}_{33}) = \begin{pmatrix} \mu_{22} & \mu_{33} \\ \mu_{11} & \mu_{11} \end{pmatrix}, B = [z^2 \rightarrow \frac{B}{h_s^3} = \bar{B}]$$

$$(\bar{Q}_{21}, \bar{Q}_{22}, \bar{Q}_{44}, \bar{Q}_{55}, \bar{Q}_{66}) = \left(\frac{Q_{21}}{Q_{11}}, \frac{Q_{22}}{Q_{11}}, \frac{Q_{44}}{Q_{11}}, \frac{Q_{55}}{Q_{11}}, \frac{Q_{66}}{Q_{11}} \right) \quad (16)$$

$$(\bar{C}_{11}, \bar{C}_{21}, \bar{C}_{22}, \bar{C}_{44}, \bar{C}_{55}, \bar{C}_{66}) = \left(\frac{C_{11}}{Q_{11}}, \frac{C_{21}}{Q_{11}}, \frac{C_{22}}{Q_{11}}, \frac{C_{44}}{Q_{11}}, \frac{C_{55}}{Q_{11}}, \frac{C_{66}}{Q_{11}} \right)$$

$$K_{bw} = \frac{K_w (2h_s + h_c)}{Q_{11}}, \quad K_{bg} = \frac{K_g}{a Q_{11}}$$

The equations of motion are obtained by setting the coefficient δU , δV , δW , $\delta \theta_1$, $\delta \theta_2$, $\delta \varphi$, $\delta \psi$ equal to zero as follows

$$\begin{aligned} \delta \theta_1 = \delta \theta_{1core} + \delta \theta_{1sheet} = & (\bar{Q}_{21} \bar{B} \alpha_s \beta_s \frac{\partial^2}{\partial \eta \partial \zeta} \theta_2 \\ & - 1/2 \bar{Q}_{44} \bar{B} \alpha_s \beta_s \frac{\partial^2}{\partial \eta \partial \zeta} \theta_2 - \bar{B} \alpha_s^2 \frac{\partial^2}{\partial \zeta^2} \theta_1 - 1/2 \bar{Q}_{44} \bar{B} \beta_s^2 \frac{\partial^2}{\partial \eta^2} \theta_1 \\ & + 1/2 \bar{Q}_{55} \alpha_c \delta \frac{\partial}{\partial \zeta} w_0 + 1/2 \bar{Q}_{55} \delta \theta_1 - 1/4 \lambda \delta \frac{\partial}{\partial \zeta} \bar{\varphi} \\ & - \bar{B} \bar{C}_{11} \alpha_s^2 \bar{\rho} \frac{\partial^2}{\partial \tau^2} \theta_1)_{core} + (-\bar{B} \bar{C}_{44} \alpha_s \beta_s \frac{\partial^2}{\partial \eta \partial \zeta} \theta_2 \\ & - 2 \bar{B} \bar{C}_{21} \alpha_s \beta_s \frac{\partial^2}{\partial \eta \partial \zeta} \theta_2 + \bar{C}_{55} \alpha_s \frac{\partial}{\partial \zeta} w_0 - 2 \bar{B} \bar{C}_{11} \alpha_s^2 \frac{\partial^2}{\partial \zeta^2} \theta_1 + \bar{C}_{55} \theta_1 \\ & - \bar{B} \bar{C}_{44} \beta_s^2 \frac{\partial^2}{\partial \eta^2} \theta_1 - 1/2 \bar{C}_{11} \frac{\partial}{\partial \zeta} \bar{\psi} - 2 \bar{B} \bar{C}_{11} \alpha_s^2 \frac{\partial^2}{\partial \tau^2} \theta_1)_{sheet} \end{aligned} \quad (17)$$

$$\begin{aligned} \delta \theta_2 = \delta \theta_{2core} + \delta \theta_{2sheet} = & (-\bar{B} \bar{Q}_{21} \alpha_s \beta_s \frac{\partial^2}{\partial \eta \partial \zeta} \theta_1 \\ & - 1/2 \bar{B} \bar{Q}_{44} \alpha_s \beta_s \frac{\partial^2}{\partial \eta \partial \zeta} \theta_1 - 1/2 \bar{B} \bar{Q}_{44} \alpha_s^2 \frac{\partial^2}{\partial \zeta^2} \theta_2 \\ & - \bar{B} \bar{Q}_{22} \beta_s^2 \frac{\partial^2}{\partial \eta^2} \theta_2 + 1/2 \bar{Q}_{66} \delta \theta_2 + 1/2 \bar{Q}_{66} \delta \beta_c \frac{\partial}{\partial \eta} w_0 \\ & - \bar{B} \bar{C}_{11} \alpha_s^2 \bar{\rho} \frac{\partial^2}{\partial \tau^2} \theta_2)_{core} + (-\bar{B} \bar{C}_{44} \alpha_s \beta_s \frac{\partial^2}{\partial \eta \partial \zeta} \theta_1 \\ & - 2 \bar{B} \bar{C}_{21} \alpha_s \beta_s \frac{\partial^2}{\partial \eta \partial \zeta} \theta_1 + \bar{C}_{66} \beta_s \frac{\partial}{\partial \eta} w_0 - 2 \bar{B} \bar{C}_{22} \beta_s^2 \frac{\partial^2}{\partial \eta^2} \theta_2 + \bar{C}_{66} \theta_2 \\ & - \bar{B} \bar{C}_{44} \alpha_s^2 \frac{\partial^2}{\partial \zeta^2} \theta_2 - 2 \bar{B} \bar{C}_{11} \alpha_s^2 \frac{\partial^2}{\partial \tau^2} \theta_2)_{sheet} \end{aligned} \quad (18)$$

$$\delta U = \delta U_{core} + \delta U_{sheet} = (-1/2 \bar{Q}_{44} \alpha_c \frac{\partial^2}{\partial \eta \partial \zeta} v_0$$

$$- \bar{Q}_{21} \alpha_c \frac{\partial^2}{\partial \eta \partial \zeta} v_0 - 1/2 \bar{Q}_{44} \gamma \beta_c \frac{\partial^2}{\partial \eta^2} u_0$$

$$- \alpha_c \frac{\partial^2}{\partial \zeta^2} u_0 + 1/4 \beta_c \gamma \frac{\partial^2}{\partial \eta^2} \bar{\varphi} - \bar{C}_{11} \alpha_c \bar{\rho} \frac{\partial^2}{\partial \tau^2} u_0)_{core}$$

$$+ (-2 \bar{C}_{11} \alpha_s^2 \frac{\partial^2}{\partial \zeta^2} u_0 - 2 \bar{C}_{21} \alpha_s \frac{\partial^2}{\partial \eta \partial \zeta} v_0$$

$$- \bar{C}_{44} \alpha_s \frac{\partial^2}{\partial \eta \partial \zeta} v_0 - \bar{C}_{44} \beta_s \gamma \frac{\partial^2}{\partial \eta^2} u_0$$

$$+ 1/2 \bar{C}_{11} \psi \beta_s \gamma \frac{\partial^2}{\partial \eta^2} \bar{\psi} - 2 \bar{C}_{11} \alpha_s \frac{\partial^2}{\partial \tau^2} u_0)_{sheet} \quad (19)$$

$$\begin{aligned} \delta V = \delta V_{core} + \delta V_{sheet} = & (-1/2\bar{Q}_{44}\alpha_c\gamma\frac{\partial^2}{\partial\eta\partial\zeta}u_0 \\ & -1/4\beta_c\frac{\partial^2}{\partial\eta\partial\zeta}\bar{\varphi}-\bar{Q}_{21}\beta_c\frac{\partial^2}{\partial\eta\partial\zeta}u_0 \\ & -1/2\frac{\bar{Q}_{44}\alpha_c\frac{\partial^2}{\partial\zeta^2}v_0}{\gamma}-\bar{Q}_{22}\beta_c\frac{\partial^2}{\partial\eta^2}v_0-\frac{\bar{C}_{11}\alpha_c\bar{\rho}\frac{\partial^2}{\partial\tau^2}v_0}{\gamma})_{core} \end{aligned} \quad (20)$$

$$\begin{aligned} & +(-2\bar{C}_{21}\beta_s\frac{\partial^2}{\partial\eta\partial\zeta}u_0-\bar{C}_{44}\beta_s\frac{\partial^2}{\partial\eta\partial\zeta}u_0-\frac{\bar{C}_{44}\alpha_s\frac{\partial^2}{\partial\zeta^2}v_0}{\gamma} \\ & -2\bar{C}_{22}\beta_s\frac{\partial^2}{\partial\eta^2}v_0+1/2\bar{C}_{11}\psi\beta_s\frac{\partial^2}{\partial\eta\partial\zeta}\bar{\psi}-2\frac{\bar{C}_{11}\alpha_s\frac{\partial^2}{\partial\tau^2}v_0}{\gamma})_{sheet} \\ \delta W = \delta W_{core} + \delta W_{sheet} = & (-1/2\bar{Q}_{55}\alpha_c\alpha_s\frac{\partial^2}{\partial\zeta^2}w_0 \\ & -1/2\bar{Q}_{66}\beta_c\beta_s\frac{\partial^2}{\partial\eta^2}w_0+1/4\lambda\alpha_c\frac{\partial^2}{\partial\zeta^2}\bar{\varphi}-1/2\bar{Q}_{55}\alpha_c\frac{\partial}{\partial\zeta}\theta_1 \\ & -1/2\bar{Q}_{66}\beta_c\frac{\partial}{\partial\zeta}\theta_2-\bar{C}_{11}\alpha_c^2\bar{\rho}\frac{\partial^2}{\partial\tau^2}w_0)_{core}+(-\bar{C}_{66}\beta_s\frac{\partial}{\partial\eta}\theta_2 \end{aligned} \quad (21)$$

$$\begin{aligned} & -\bar{C}_{55}\alpha_s\frac{\partial}{\partial\zeta}\theta_1-\bar{C}_{66}\beta_s^2\frac{\partial^2}{\partial\eta^2}w_0-\bar{C}_{55}\alpha_s^2\frac{\partial^2}{\partial\zeta^2}w_0 \\ & +1/2\bar{C}_{11}\alpha_s\frac{\partial^2}{\partial\zeta^2}\bar{\psi}-2\bar{C}_{11}\alpha_s^2\frac{\partial^2}{\partial\tau^2}w_0)_{sheet} \\ \delta\varphi = & (1/4\alpha_c\frac{\partial^2}{\partial\eta\partial\zeta}v_0+1/4\lambda\alpha_c\alpha_s\frac{\partial^2}{\partial\zeta^2}w_0 \\ & +1/4\lambda\alpha_c\frac{\partial}{\partial\zeta}\theta_1+1/4\gamma\beta_c\frac{\partial^2}{\partial\eta^2}u_0+g\alpha_c\frac{\partial^2}{\partial\zeta^2}\bar{\varphi} \\ & -1/4\lambda\alpha_c^2\frac{\partial^2}{\partial\zeta^2}w_0-1/4\lambda\alpha_c\frac{\partial}{\partial\zeta}\theta_1+g\bar{\sigma}_{22}\gamma\beta_c\frac{\partial^2}{\partial\eta^2}\bar{\varphi} \\ & -1/4\alpha_c\frac{\partial^2}{\partial\eta\partial\zeta}v_0-1/4\beta_c\gamma\frac{\partial^2}{\partial\eta^2}u_0) \end{aligned} \quad (22)$$

$$\begin{aligned} \delta\psi = & (1/2\alpha_s\frac{\partial}{\partial\zeta}\theta_1+1/2\psi\beta_s\gamma\frac{\partial^2}{\partial\eta^2}u_0 \\ & +1/2\alpha_s^2\frac{\partial^2}{\partial\zeta^2}w_0+1/2\psi\alpha_s\frac{\partial^2}{\partial\eta\partial\zeta}v_0+2Y\alpha_s\frac{\partial^2}{\partial\zeta^2}\bar{\psi} \\ & -1/2\alpha_s^2\frac{\partial^2}{\partial\zeta^2}w_0-1/2\alpha_s\frac{\partial}{\partial\zeta}\theta_1+\bar{\mu}_{22}Y\gamma\beta_s\frac{\partial^2}{\partial\eta^2}\bar{\psi} \\ & -1/2\psi\alpha_s\frac{\partial^2}{\partial\eta\partial\zeta}v_0-1/2\psi\beta_s\gamma\frac{\partial^2}{\partial\eta^2}u_0) \end{aligned} \quad (23)$$

4. Solution method

To apply the DQ method, at first Eq. (24) is used to separate the time and spatial variables

$$\begin{aligned} U(\zeta,\eta,\tau) &= U(\zeta,\eta)e^{\omega\tau} \\ V(\zeta,\eta,\tau) &= V(\zeta,\eta)e^{\omega\tau} \\ W(\zeta,\eta,\tau) &= W(\zeta,\eta)e^{\omega\tau} \\ \theta_1(\zeta,\eta,\tau) &= \theta_1(\zeta,\eta)e^{\omega\tau} \\ \theta_2(\zeta,\eta,\tau) &= \theta_2(\zeta,\eta)e^{\omega\tau} \\ \psi(\zeta,\eta,\tau) &= \psi(\zeta,\eta)e^{\omega\tau} \\ \varphi(\zeta,\eta,\tau) &= \varphi(\zeta,\eta)e^{\omega\tau} \end{aligned} \quad (24)$$

where $\omega = \Omega a \sqrt{\rho_s / C_{11}}$ is the dimensionless frequency (Ω is the dimensional frequency). In DQM, the differential equations change into the first algebraic equations. In this regard, the partial derivatives of a function (F) are approximated by a specific variable, at discontinuous points by a set of weighting series. It's supposed that F be a function representing U, V, W, θ_1 and θ_2, ψ, φ with respect to variables ζ and η ($0 < \zeta < 1, 0 < \eta < 1$) when $N_\zeta \times N_\eta$ be the grid points along these variables with following derivative (Shu 2000)

$$\begin{aligned} \frac{d^n F(\zeta_i, \eta_j)}{d\zeta^n} &= \sum_{k=1}^{N_\zeta} A_{ik}^{(n)} F(\zeta_k, \eta_j) \quad n = 1, \dots, N_\zeta - 1, \\ \frac{d^m F(\zeta_i, \eta_j)}{d\eta^m} &= \sum_{l=1}^{N_\eta} B_{jl}^{(m)} F(\zeta_i, \eta_l) \quad m = 1, \dots, N_\eta - 1, \\ \frac{d^{n+m} F(\zeta_i, \eta_j)}{d\zeta^n d\eta^m} &= \sum_{k=1}^{N_\zeta} \sum_{l=1}^{N_\eta} A_{ik}^{(n)} B_{jl}^{(m)} F(\zeta_k, \eta_l) \end{aligned} \quad (25)$$

where $A_{ik}^{(n)}$ and $B_{jl}^{(m)}$ are the weighting coefficients using Chebyshev polynomials for the positions of the grid points whose recursive formulae can be found in (Shu 2000). Applying DQM and using (25) into governing (17-23), the standard form of equations of motion ($M\ddot{X} + KX = 0$) are obtained. Considering simply supported boundary conditions as follow

$$\begin{cases} W_{i1} = V_{i1} = U_{i1} = \varphi_{y1} = \psi_{y1} = 0, \\ M_{xx}|_{i1} = 0, \quad M_{xx} = \int z \sigma_{xx} dz \\ W_{Ni} = V_{Ni} = U_{Ni} = \varphi_{yNi} = \psi_{yNi} = 0, \\ M_{xx}|_{iN} = 0 \end{cases} \quad (26)$$

An eigen value problem is derived in which $\omega = \sqrt{K} / \sqrt{M}$ is introduced as the dimensionless frequency. It is worth mentioning that M is the mass matrix and K is the stiffness.

5. Numerical results and discussion

In this work, FSDT was used to derive the equations of motion of sandwich plate with composite core and piezomagnetic face sheets under variable in-plane load. The results of this study include the effect of load factor, aspect ratio, thickness ratio, boundary condition, elastic medium and material properties. The PFRC core is made of PZT-4

Table 1 Mechanical properties of matrix (Tan and Tong 2000)

	$C_{11}=(C_{22}=C_{33})GPa$	$C_{12}=(C_{13}=C_{23})GPa$	$C_{44}=(C_{55}=C_{66})GPa$	$\rho(Kg/m^3)$
Matrix	3.74	1.12	1.31	1170

Table 2 Electro-mechanical properties of $CoFe_2O_4$, $BaTiO_3$, $PZT - 4$ (Yang 2005, Ramirez 2006)

	$CoFe_2O_4$	$BaTiO_3$		$PZT - 4$
$C_{11c} = C_{22c}$ (GPa)	286	166	$Q_{11c} = Q_{22c}$ (GPa)	13.9
$C_{13c} = C_{23c}$ (GPa)	170.5	78	$Q_{13c} = Q_{23c}$ (GPa)	7.40
$C_{44c} = C_{55c}$ (GPa)	45.3	43	$Q_{44c} = Q_{55c}$ (GPa)	2.56
C_{12c} (GPa)	173	77	Q_{12c} (GPa)	7.78
C_{33c} (GPa)	269.5	162	Q_{33c} (GPa)	11.5
C_{66c} (GPa)	56.5	44.5	Q_{66c} (GPa)	3.06
$q_{31}(N/Am)$	580.3	-4.4	$e_{31}(C/m^2)$	-5.2
$q_{32}(N/Am)$	580.3	-4.4	$e_{32}(C/m^2)$	0
$q_{33}(N/Am)$	699.7	18.6	$e_{33}(C/m^2)$	15.1
$q_{24}(N/Am)$	550	11.6	$e_{24}(C/m^2)$	0
$q_{15}(N/Am)$	550	11.6	$e_{15}(C/m^2)$	12.7
$\epsilon_{11} (*10^{-8}C/Vm)$	0.080	11.2	ϵ_{11}	0.0646
ϵ_{22}	0.080	11.2	ϵ_{22}	0
ϵ_{33}	0.093	12.6	ϵ_{33}	0.562
$\mu_{11} (10^{-6}Ns^2/C^2)$	-590	5		
μ_{22}	-590	5		
μ_{33}	157	10		
$\rho (Kg/m^3)$	5300	5800	$\rho (Kg/m^3)$	7500

fibers and material properties of matrix have been listed in Table 1. Also, Table 1 and Table 2 reports the properties of $CoFe_2O_4$ and $BaTiO_3$ as face sheets.

At first, to ensure the correct results, linear frequency $\omega = \Omega a^2 \sqrt{\rho h/D}$, $D = EI/(1-\nu^2)$ for an isotropic square plate are compared in Table 3 for two modes. A good agreement among the results of present work and other published papers (Loja 2013, Bardell 1989, Wang *et al.* 2004) shows that the correct solution has been used.

It is worth to mention that although the dynamic problem can be coupled with the stability problem, this coupling it is not the goal of the present work.

The results of this research are presented in six sections:

- Effect of volume fraction of fibers
- Effect of thickness and aspect ratios (geometric

Table 1 Comparison of linear frequency for an isotropic square plate ($\gamma = 1$, $\beta = 1/300$, $\nu = 0.3$)

	ω_1	ω_2
Bardell (1989)	19.7392	49.3480
Wang <i>et al.</i> (2004)	19.7392	49.3453
Wang and Shen (2012)	19.7362	49.3431
Present work	19.4250	49.3392

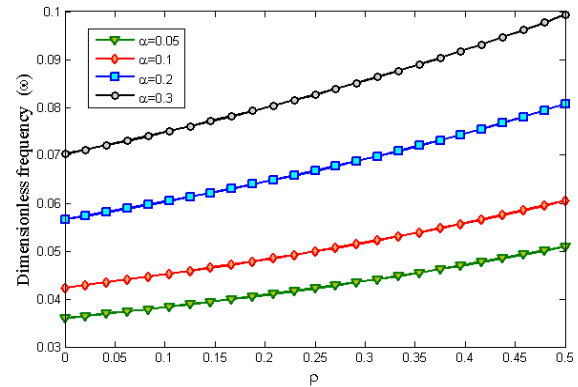


Fig. 3 Variation of dimensionless frequency versus volume fraction of fibers in composite core

parameters)

- Effect of boundary conditions
- Different load factor
- Effect of elastic medium
- Effect of material properties

Fig. 3 shows the effect of volume fraction of fibers on dimensionless frequency of sandwich plate for different value of core thickness ratios. It can be seen from the figure that dimensionless frequency (ω) increases with increasing the volume fraction of fibers (ρ), because fibers reinforce the strength of composite, significantly.

A plate is a structural element which is thin and flat. When the plate's transverse dimension, or thickness, is small in comparison with the length and width dimensions, the plate is thin. A mathematical expression of this idea is $h/a \ll 1$;

Plates are classified based on the thickness ratio as follows (Steele and Balch 2009):

- very thin: $h/a < 0.01$,
- moderately thin: $0.01 < h/a < 0.05$,
- thick: $0.05 < h/a < 0.3$,
- very thick: $h/a > 0.3$.

Classical theory of plates is applicable to very thin and moderately thin plates, while HSDT for thick plates are useful. FSDT with five unknown displacements has been used for thin and thick plates frequently. For the very thick plates, however, it becomes more difficult and less useful to view the structural element as a plate, a description based on the three-dimensional theory of elasticity is required.

Fig. 3 also shows that increasing α_c leads to increase the dimensionless frequency for all ranges of thin and thick plates.

Effect of different boundary conditions on frequency response of sandwich plate has been displayed in Fig. 4.

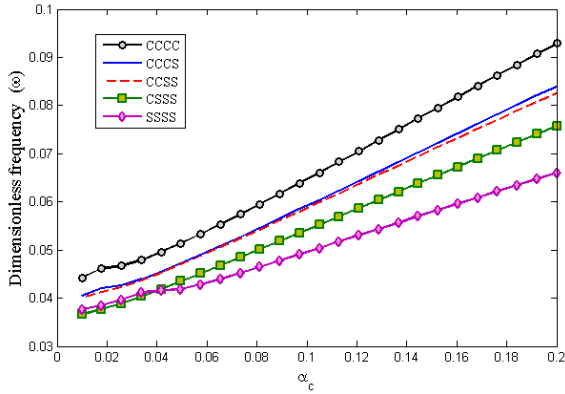


Fig. 4 Variation of dimensionless frequency versus core thickness ratio α_c for various cases of the boundary conditions

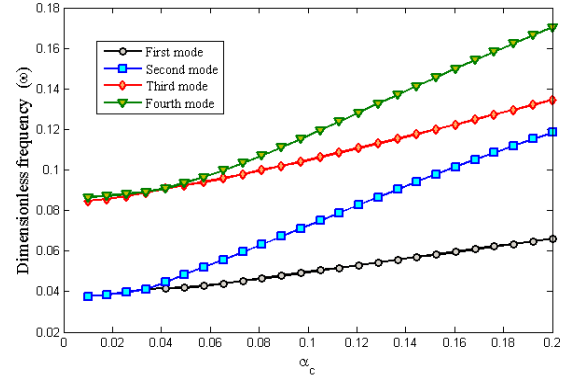


Fig. 6 Variation of dimensionless frequency versus core thickness ratio α_c in four primary modes

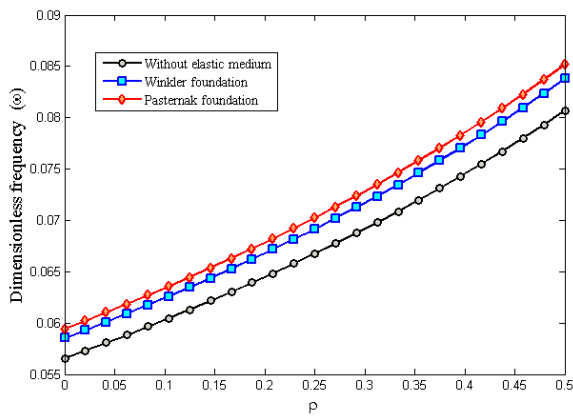


Fig. 5 Effect of elastic medium on vibration frequency of sandwich plate

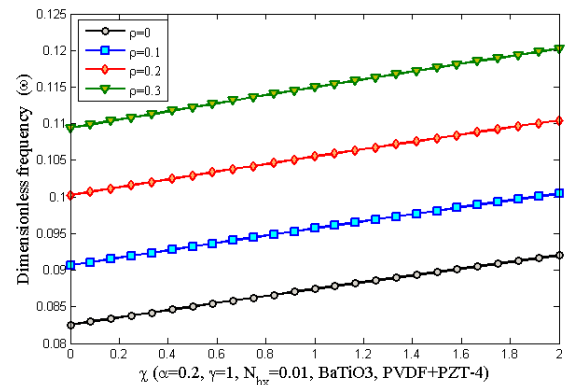


Fig. 7 Effect of load factor on vibration frequency of sandwich plate

Five boundary conditions of *CCCC*, *CCCS*, *CCSS*, *CSSS* and *SSSS* have been compared in this figure where the value of dimensionless frequency for *CCCC* is larger than the others. Result reveals that *CCCC* boundary condition provides maximum stability for system and minimum stability relates to *SSSS* boundary condition as follows:

$$CCCC > CCCS > CCSS > CSSS > SSSS$$

Physically, *CCCC* boundary condition increases the stiffness of sandwich and finally dimensionless frequency.

Fig. 5 shows the variation of dimensionless frequency versus volume fractions of composite core in different elastic mediums. The lowest curve reports the values of dimensionless frequency without elastic medium where ω has the minimum value to the other cases. 2th curve is belong to the Winkler foundation with spring constant K_{bw} . Pasternak foundation includes two normal and shear modules and it is more effective than Winkler type. The role of elastic medium in stability of system is observed in Fig. 5 where Pasternak modules create the larger values for natural frequency of sandwich plate. Physically the structural performance is a function of environmental conditions.

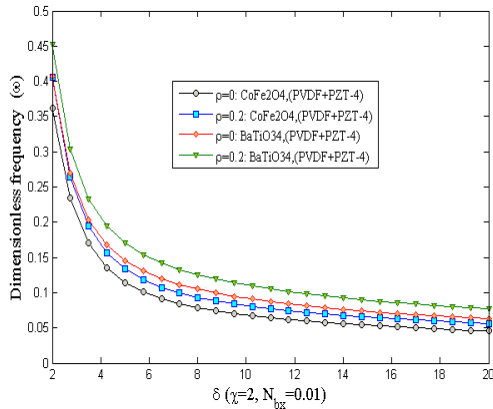
Dimensionless frequency of sandwich plate versus core thickness ratio has been displayed in Fig. 6 for four primary

modes. It is clear from the figure that the first and second modes have the same values until $\alpha_c \approx 0.035$ and, also third and fourth modes have overlap in $0.01 \leq \alpha_c \leq 0.04$. Therefore, it is important to structure what is vibrating mode because the structural performance is different in different modes.

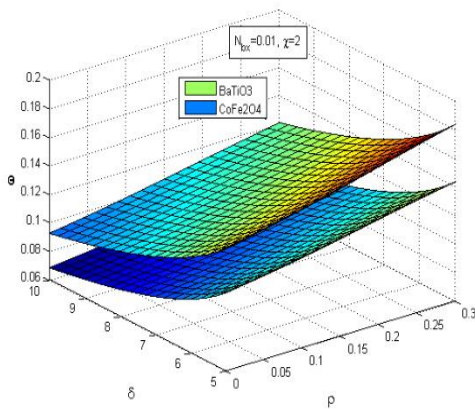
In order to clarify the effects of different load factors on the vibration frequency of sandwich plate, Fig. 7 has been drawn. In this figure, *PVDF* has been selected as matrix of composite. The mechanical properties of *PVDF* are reported in Ref. (Ghorbanpour Arani *et al.* 2015). It is found that the dimensionless frequency increases with increasing of load factor in $0 \leq \chi \leq 2$. It is clear from the figure that the dimensionless frequency is more than the other cases in pure bending case ($\chi = 2$).

According to Fig. 8, dimensionless frequency of sandwich plate changes by changing of face sheets and volume fraction of fibers. *CoFe₂O₄* and *BaTi₃O₄* are selected as face sheets, *PVDF* as matrix and *PZT-4* as reinforcing fibers of composite core to study the effect of material properties. *CoFe₂O₄* and *BaTi₃O₄* are piezomagnetic materials and review of elastic properties in Table 2 approves the result of Fig. 8.

Given the variety of piezoelectric and piezomagnetic materials, their vibration behavior depends on the material properties and the kind of materials can alter the frequency domain.



(a)



(b)

Fig. 8 Variation of dimensionless frequency (a) versus $\delta=h_c/h_f$ in different materials. (b) versus δ and ρ in different materials

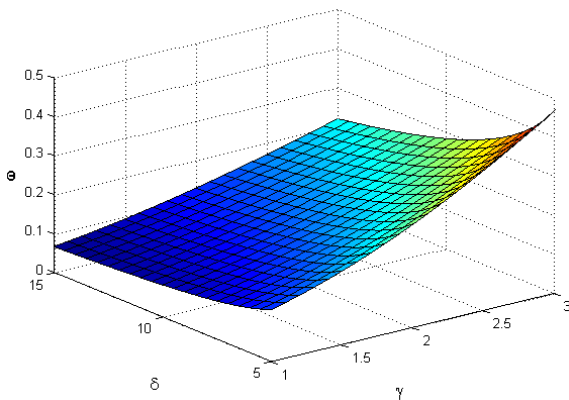


Fig. 9 Variation of dimensionless frequency versus aspect ratio $\gamma=a/b$ and δ

Fig. 9 illustrates the variation of dimensionless frequency of sandwich plate with core of *PVDF+PZT-4* and face sheets of *BaTi₃O₄* versus aspect ratio $\gamma=a/b$ and δ . It's clear from the figure that increasing the aspect ratio $\gamma=1$ to 3 leads to growth of dimensionless frequency while increasing δ has reverse effect. Comparison between elastic properties of composite core and face sheets reveals that

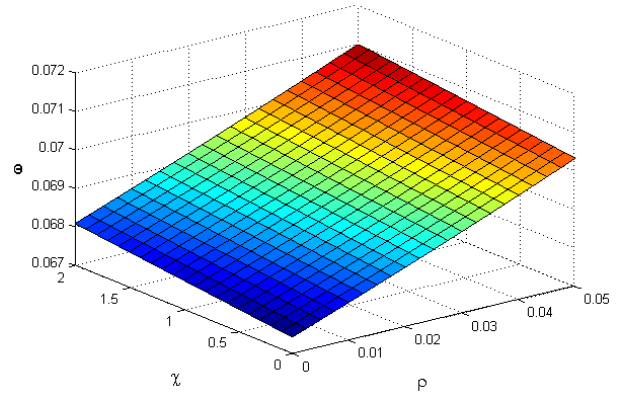


Fig. 10 Variation of dimensionless frequency versus load factor and volume fraction of fibers

effective electroelastic constants for PFRC is lower than *BaTi₃O₄*. So, with increasing core to face thickness (δ), the dimensionless frequency decreases.

Fig. 10 shows the simultaneous effect of load factor and volume fraction of fibers on dimensionless frequency of sandwich plate with core of *PVDF+PZT-4* and face sheets of *BaTi₃O₄*. As increase of volume fraction of fibers leads to increase of dimensionless frequency, increasing of load factor has the same effect.

6. Conclusions

Free vibration of sandwich plate with PFRC core and piezomagnetic face sheets is a novel topic that has been studied in this research. Composite core was reinforced by piezoelectric fibers and micromechanical approach was applied to estimate the effective electroelastic constants of PFRC materials. Face sheets in top and bottom of composite core is made of piezomagnetic materials. Pasternak foundation was developed to evaluate the effect of normal and shear modulus on the stability of sandwich structure. Also, sandwich plate undergoes the variable in-plane forces. Set of equations were solved by two-dimensional DQM and the following results were concluded:

- Pasternak foundation plays an important role on the stability of sandwich plate where normal (k_{bw}) and shear (K_{bg}) modulus significantly increase the dimensionless frequency of sandwich plate.
- Increasing load factor from $\chi=0$ to 2, increases the dimensionless frequency of sandwich plate. Because pure compression load ($\chi=0$) changes to pure bending case ($\chi=2$).
- The selected materials for fibers, matrix and face sheets change the dimensionless frequency of sandwich plate.
- Dimensionless frequency (ω) increases with increasing the volume fraction of fibers (ρ) because, fibers reinforce the strength of composite significantly.
- Aspect ratio and thickness ratio increase the dimensionless frequency while core-to-face sheet ratio decreases ω due to change in effective electroelastic

constants of PFRC materials and face sheets properties.

The result of this study can be useful to design and manufacturing of aircraft, ships, satellites, rail cars, automobiles and other industries.

Acknowledgments

The authors would like to thank the reviewers for their comments and suggestions to improve the clarity of this article. This work was supported by University of Kashan [grant number 574600/19].

References

- An, C. and Su, J. (2014), "Dynamic analysis of axially moving orthotropic plates: Integral transform solution", *Appl. Math. Comput.*, **228**, 489-507.
- Araújo, A. and Mota Soares, C. (2010), "A viscoelastic sandwich finite element model for the analysis of passive, active and hybrid structures", *Appl. Compos. Mater.*, **17**(5), 529-542.
- Aravinda Kumar, M.S., Panda, S. and Chakraborty, D. (2015), "Design and analysis of a smart graded fiber-reinforced composite laminated plate", *Compos. Struct.*, **124**, 176-195.
- Bardell, N.S. (1989), "The application of symbolic computing to the hierarchical finite element method", *Int. J. Numer. Meth. Eng.*, **28**(5), 1181-1204.
- Belabed, Z., Houari, M.S.A., Tounsi, A., Mahmoud, S.R. and Anwar Bég, O. (2014), "An efficient and simple higher order shear and normal deformation theory for functionally graded material (FGM) plates", *Compos. Part B-Eng.*, **60**, 274-283.
- Benjeddou, A. and Deü, J.F. (2002), "A two-dimensional closed-form solution for the free-vibrations analysis of piezoelectric sandwich plates", *Int. J. Solids. Struct.*, **39**(6), 1463-1486.
- Bessaim, A., Houari, M.S., Tounsi, A., Mahmoud, S.R. and Bedia, E.A.A. (2013), "A new higher-order shear and normal deformation theory for the static and free vibration analysis of sandwich plates with functionally graded isotropic face sheets", *J. Sandw. Struct. Mater.*, **15**(6), 671-703.
- Cook, A.C. and Vel, S.S. (2012), "Multiscale analysis of laminated plates with integrated piezoelectric fiber composite actuators", *Compos. Struct.*, **94**(2), 322-336.
- Farajpour, A., Shahidi, A.R., Mohammadi, M. and Mahzoon, M. (2012), "Buckling of orthotropic micro/nanoscale plates under linearly varying in-plane load via nonlocal continuum mechanics", *Compos. Struct.*, **94**(5), 1605-1615.
- Ghorbanpour Arani, A. and Khoddami Maraghi, Z. (2016), "A feedback control system for vibration of magnetostrictive plate subjected to follower force using sinusoidal shear deformation theory", *Ain Shams Eng. J.*, **94**(15), 361-369.
- Ghorbanpour Arani, A., Vossough, H., Kolahchi, R. and Mosallaie Barzoki, A.A. (2012), "Electro-thermo nonlocal nonlinear vibration in an embedded polymeric piezoelectric micro plate reinforced by DWBNTs using DQM", *J. Mech. Sci. Technol.*, **26**(10), 3047-3057.
- Ghorbanpour Arani, A., Haghparast, E., Heidari Rarani, M. and Khoddami Maraghi, Z. (2015), "Strain gradient shell model for nonlinear vibration analysis of visco-elastically coupled Boron Nitride nano-tube reinforced composite micro-tubes conveying viscous fluid", *Comp. Mater. Sci. (Part B)*, **96**, 448-458.
- Houari, M.S.A., Tounsi, A. and Anwar Beg, O. (2013), "Thermoelastic bending analysis of functionally graded sandwich plates using a new higher order shear and normal deformation theory", *Int. J. Mech. Sci.*, **76**, 102-111.
- Jalili, N. (2010), *Piezoelectric-Based Vibration Control: From Macro to Micro/Nano Scale Systems*, Springer. 536.
- Khalili, S.M.R., Kheirikhah, M.M. and Malekzadeh Fard, K. (2014), "Biaxial wrinkling analysis of composite-faced sandwich plates with soft core using improved high-order theory", *Eur. J. Mech. A. Solid.*, **43**, 67-77.
- Kutlu, A. and Hakk Omurtag, M. (2012), "Large deflection bending analysis of elliptic plates on orthotropic elastic foundation with mixed finite element method", *Int. J. Mech. Sci.*, **65**(1), 64-74.
- Lal, R. and Rani, R. (2014), "On the use of differential quadrature method in the study of free axisymmetric vibrations of circular sandwich plates of linearly varying thickness", *J. Vib. Control*, **22**(7), 1729-1748.
- Lee, K.H., Wang, C.M. and Reddy, J.N. (2000), *Shear Deformable Beams and Plates*, Elsevier Science Ltd: Oxford. 279-291.
- Li, Q., Iu, V.P. and Kou, K.P. (2008), "Three-dimensional vibration analysis of functionally graded material sandwich plates", *J. Sound. Vib.*, **311**(1-2), 498-515.
- Loja, M.A.R., Mota Soares, C.M. and Barbosa, J.I. (2013), "Analysis of functionally graded sandwich plate structures with piezoelectric skins, using B-spline finite strip method", *Compos. Struct.*, **96**, 606-615.
- Mallick, P.K. (2007), *Fiber reinforced composites Materials, Manufacturing, and Design*, Taylor & Francis Group, 616.
- Natarajan, S., Haboussi, M. and Manickam, G. (2014), "Application of higher-order structural theory to bending and free vibration analysis of sandwich plates with CNT reinforced composite facesheets", *Compos. Struct.*, **113**, 197-207.
- Nayak, A.K., Moy, S.S.J. and Shenoi, R.A. (2002), "Free vibration analysis of composite sandwich plates based on Reddy's higher-order theory", *Compos. Part B-Eng.*, **33**(7), 505-519.
- Plagianakos, T.S. and Papadopoulos, E.G. (2015), "Higher-order 2-D/3-D layerwise mechanics and finite elements for composite and sandwich composite plates with piezoelectric layers", *Aerosp. Sci. Technol.*, **40**, 150-163.
- Ramirez, F., Heyliger, P.R. and Pan, E. (2006), "Discrete layer solution to free vibrations of functionally graded magneto-electro-elastic plates", *Mech. Adv. Mater. Struct.*, **13**(3), 249-266.
- Reddy, J.N. (2002), *Energy Principles and Variational Methods in Applied Mechanics*, 2nd Edition, in Energy Principles and Variational Methods in Applied Mechanics, 2nd Edition. WILEY. 592.
- Shu, C. (2000), *Differential Quadrature and its Application in Engineering*, Springer publishers Singapore.
- Steele, C.R. and Balch, C.D. (2009), "Introduction to the theory of plates", Stanford University.
- Tan, P. and Tong, L. (2001), "Micromechanics models for non-linear behavior of piezo-electric fiber reinforced composite materials", *Int. J. Solids. Struct.*, **38**(50-51), 8999-9032.
- Tan, P. and Tong, L. (2002), "Investigation of loading assumptions on the effective electroelastic constants for PFRC materials", *Compos. Struct.*, **57**(1-4), 101-108.
- Tan, P. and Tong, L. (2002), "Modeling for the electro-magneto-thermo-elastic properties of piezoelectric-magnetic fiber reinforced composites", *Compos. Part A-Appl. S.*, **33**(5), 631-645.
- Tounsi, A., Houari, M.S.A., Benyoucef, S. and Adda Bedia, E.A. (2013), "A refined trigonometric shear deformation theory for thermoelastic bending of functionally graded sandwich plates", *Aerosp. Sci. Technol.*, **24**, 209-220.
- Tu, T.M., Thach, L.N. and Quoc, T.H. (2010), "Finite element modeling for bending and vibration analysis of laminated and sandwich composite plates based on higher-order theory", *Comput. Mater. Sci.*, **49**(4), 390-394.
- Wang, T., Sokolinsky, V., Rajaram, S. and Nutt, S.R. (2008),

- “Consistent higher-order free vibration analysis of composite sandwich plates”, *Compos. Struct.*, **82**(4), 609-621.
- Wang, Y., Wang, X. and Zhou, Y. (2004), “Static and free vibration analyses of rectangular plates by the new version of the differential quadrature element method”, *Int. J. Numer. Meth. Eng.*, **59**(9), 1207-1226.
- Wang, Z.X. and Shen, H.S. (2012), “Nonlinear vibration and bending of sandwich plates with nanotube-reinforced composite face sheets”, *Compos. Part B-Eng.*, **43**(2), 411-421.
- Yang, J. (2005), *An Introduction to the Theory of Piezoelectricity*, Springer US. 309.
- Zhang, X.D. and Sun, C.T. (1999), “Analysis of a sandwich plate containing a piezoelectric core”, *Smart. Mater. Struct.*, **8**(1), 31.

CC

Abbreviation

PFRC	piezoelectric fiber reinforced composite core
FSDT	first order shear deformation theory
DQM	differential quadrature method
2D	two-dimensional
PEMFRC	piezoelectric-magnetic fiber reinforced composite
PVC	poly-vinyl-chloride
FGM	functionally graded material
FG	functionally graded
HSDT	higher order shear deformation theory
CNTRC	carbon nanotube-reinforced composite
CNT	carbon nanotube
RVE	representative volume element
CPT	classical plate theory